

Peculiarity of highly radiating multi-impurity seeded *H*-mode plasmas on JET with ITER-like wall

A Huber¹ , M Wischmeier², M Bernert², S Wiesen¹ , S Glöggler², S Aleiferis³, S Brezinsek¹ , G Calabro⁴, P Carvalho⁵, V Huber⁶ , G Sergienko¹, E R Solano⁷, C Giroud⁸, M Groth⁹, S Jachmich¹⁰, Ch Linsmeier¹ , G F Matthews⁸, A G Meigs⁸, Ph Mertens¹ , M Sertoli², S Silburn⁸, G Telesca¹¹ and JET contributors¹²

¹Forschungszentrum Jülich GmbH, Institut für Energie- und Klimaforschung—Plasmaphysik, Partner of the Trilateral Euregio Cluster (TEC), D-52425 Jülich, Germany

²Max-Planck-Institut für Plasmaphysik, Boltzmannstraße 2, D-85748 Garching, Germany

³NCSR ‘Demokritos’, 153 10, Agia Paraskevi Attikis, Greece

⁴Department of Economics, Engineering, Society and Business Organization (DEIm), University of Tuscia, Largo dell’Università snc, I-01100 Viterbo, Italy

⁵Instituto de Plasmas e Fusão Nuclear, Instituto Superior Técnico, Universidade de Lisboa, Portugal

⁶Forschungszentrum Jülich GmbH, Supercomputing Centre, D-52425 Jülich, Germany

⁷Laboratorio Nacional de Fusión, CIEMAT, Madrid, Spain

⁸CCFE, Culham Science Centre, Abingdon, OX14 3DB, United Kingdom

⁹Aalto University, Association EURATOM-Tekes, PO Box 4100, FI-2015 Espoo, Finland

¹⁰Laboratory for Plasma Physics, ERM/KMS, B-1000 Brussels, Belgium

¹¹Institute of Plasma Physics and Laser Microfusion, Warsaw, Poland

E-mail: A.Huber@fz-juelich.de

Received 21 June 2019, revised 15 October 2019

Accepted for publication 13 November 2019

Published 16 March 2020



CrossMark

Abstract

On JET with fully metallic first wall, highly radiative conditions with N₂, Ne and Ar as well as their mixture as radiators are approached in high density *H*-mode plasmas. The confinement increases from $H_{98(y,2)} = 0.65$ in unseeded pulses with $\gamma_{\text{rad}} \sim 30\%$ to a value of $H_{98(y,2)} = 0.75$ at $\gamma_{\text{rad}} \sim 50\%$ with N₂ injection. A degradation of the pedestal profile is compensated by steeper core n_e and T_e profiles. Further increase of γ_{rad} with increase of the N₂ seeding rate leads to a moderate confinement degradation which can be avoided by applying of combined impurity seeding. The enhancement of the plasma performance for the radiation fractions beyond 55% with the maximum value of $H_{98(y,2)} = 0.78$ is reached with combined N₂ + Ne and N₂ + Ar impurity injections. The observed intense, strongly localized radiation at the *X*-point inside the confined plasma in the scenarios with the highest radiated power fraction is interlinked to complete divertor detachment. In the JET-ILW, the *X*-point radiation is stable, reproducible and reversible.

Keywords: power exhaust, radiation, impurities in plasmas, divertors, detachment, tokamaks

(Some figures may appear in colour only in the online journal)

1. Introduction

The development of plasma scenarios with high fractions of radiated power through impurity seeding is essential for the safe operation of future fusion devices with a burning plasma such as

¹² See the author list of E Joffrin *et al* accepted for publication in Nuclear Fusion Special issue 2019, <https://doi.org/10.1088/1741-4326/ab2276>.

ITER and DEMO where perpendicular divertor target loads should be kept below $5\text{--}10\text{ MW m}^{-2}$ [1, 2] to avoid divertor damage. At the same time, the electron temperature at the target needs to be low enough to restrict the erosion of the divertor to acceptable levels. However, radiative power losses within the confined plasma can affect the plasma confinement and fuel dilution as well as the discharge stability. Therefore, it is very important to understand underlying physical processes in highly radiative discharges to provide the recipe for controlled seeding with a reasonable reduction in the power flux and target temperature while minimizing the impact on the confined plasma.

Consequently, the selection of an extrinsic impurity for fusion devices is based on its radiative characteristics in the regions of divertor and main plasma as well as on their influence on plasma confinement under high divertor radiation conditions. Also the interaction of the seeded impurities with the plasma-facing components, which affects the tritium processing plant, should be taken into account. In the present tokamak experiments nitrogen is favoured as divertor radiator since it is more efficiently compressed than Ne. At the same time N_2 provides adequately localized divertor radiation [3–5]. However, nitrogen is chemically active and can cause the formation of ammonia. During the ITER operation with the Deuterium–Tritium fuel mix and N_2 impurity seeding, a tritiated ammonia (NT_3) will be produced [6]. The amount of NT_3 produced may be significant and could have an impact on the exhaust treatment, which will affect the design of the ITER tritium plant. In contrast to the experimental observations, simulations of ITER plasmas at high performance [7] show that compression for N_2 and Ne will be similar. In addition, Ne is not chemically reactive, which makes it an attractive candidate as a divertor radiator in ITER. In addition to N_2 and Ne, argon is considered also as a further candidate for simultaneous improvement of core and divertor radiation, when some increased radiation in the main chamber is requested. It is assumed that adequate divertor compression for Ar can be achieved.

Impurities, such as neon (Ne), nitrogen (N_2) and argon (Ar) are commonly used in experiments with strongly radiative divertor on many tokamaks [8–10]. On the other hand, interpretation studies on mixed seed discharges in tokamaks have not been performed very often [11, 12]. Therefore, further investigations on mixed seeding experiments must be performed to develop scenarios with a reasonable energy confinement simultaneously with a high level of radiation.

2. Impurity seeding in high-density *H*-mode plasmas

2.1. N_2 seeding in high density *H*-mode plasmas

After the first wall of JET was upgraded to an ITER-like wall (ILW) [13], the level of carbon was reduced at least by a factor of 10 [14] leading to a strong reduction of the divertor radiation in the fully metallic machine.

Nitrogen proves to be an appropriate replacement for carbon as a divertor radiator thanks to its maximum radiative

efficiency at low temperatures, $T_e \sim 10\text{--}20\text{ eV}$ [15]. Dedicated *H*-mode nitrogen seeding experiments have been carried out at JET with the ITER-like wall (JET-ILW) to study the impact of seeding with diverse impurities on the energy confinement. In addition, the influence of different impurity species on the balance between radiation in the divertor region and in the main chamber has been investigated. High density Type I ELMy *H*-mode plasmas at $B_T = 2.7\text{ T}$, $I_p = 2.5\text{ MA}$ ($q_{95} = 3.3$) at Greenwald density fraction $f_{\text{GW}} (= \langle n_e \rangle / n_{e,\text{GW}})$ up to 85% in low-triangularity magnetic equilibria ($\delta = 0.22$) with both strike points on the lower vertical targets have been examined. Thereby, the Greenwald density limit $n_{e,\text{GW}} [10^{20}\text{ m}^{-3}] = I_p [\text{MA}] / (\pi a^2)$ and a is the plasma minor radius in m [16]. Respective scans have been performed over a deuterium fuelling range of $2 \times 10^{22}\text{ el s}^{-1} \div 6.5 \times 10^{22}\text{ el s}^{-1}$ and an impurity seeding range of $2 \times 10^{22}\text{ el s}^{-1} \div 1.3 \times 10^{23}\text{ el s}^{-1}$ with an auxiliary heating power of 18 MW. Fuelling and seeding rate are given in this contribution in unit of electrons per second (el s^{-1}) due to the complete ionisation of the injected gas flow. The emission signal of beryllium in the outer divertor (Be II 527 nm) with high temporal resolution (10 kHz) represents the behaviour of ELMs. Opposite to an unseeded plasma (not shown in the figure), the radiation scenario with N_2 seeding shows small energy ELMs directly after the *L*–*H* transition, with a fast transition at 10.8 s from a Type I ELMy to a stable and stationary ELM-free *H*-mode phase.

The N_2 gas has been injected into the private flux region (PFR) of the outer divertor leg with seeding rate of $\Gamma_{\text{N}_2} \approx 13.4 \times 10^{22}\text{ el s}^{-1}$. The ELM-free *H*-mode phase demonstrates cold pedestal ($T_e^{\text{ped}} \approx 300\text{ eV}$) and some recovery of the energy confinement (figure 1(a)). During this ELM free *H*-mode, the so-called *M*-mode [17] with plasma performance between *L*-mode and *H*-mode (medium confinement), the radiation fraction reaches the value of $\gamma_{\text{rad}} \sim 75\%$. This mode can typically be observed during the operation with the input power close to the *L*–*H* power threshold or just right after an *L*–*H* transition. During the *M*-mode phase the characteristic oscillation can be seen in the fast divertor D_α emissions as well as in the signals of a poloidal Mirnov coil.

In the unseeded plasma, the global confinement was significantly degraded at higher fuelling rate required to reach a high density close to Greenwald limit [16]. In comparison with the unseeded pulse, the ion effective charge Z_{eff} increases during the N_2 seeding by $\approx 50\%$ from 1.1 to 1.7 (increase of $\Delta Z_{\text{eff}} = 0.6$). The radiation fraction in this pulse reaches its peak-value of about 75%. Considerable energy confinement recovery is observed with N_2 seeding. It increases from a confinement factor of $H_{98(y,2)} = 0.65$ in the pulse with D_2 fuelling only to a factor of $H_{98(y,2)} = 0.75$. Figure 1(b) shows profiles of the electron temperature (T_e) and density (n_e) measured by the High Resolution Thomson Scattering system [18] in unseeded as well as seeded plasmas. Contrary to the case of unseeded plasma, the electron density n_e in the nitrogen seeded plasmas decreases in the edge region and increases in the plasma core correspondingly, demonstrating a more significantly peaked behaviour (see figure 1(b)). This steepening is explained using ASTRA-

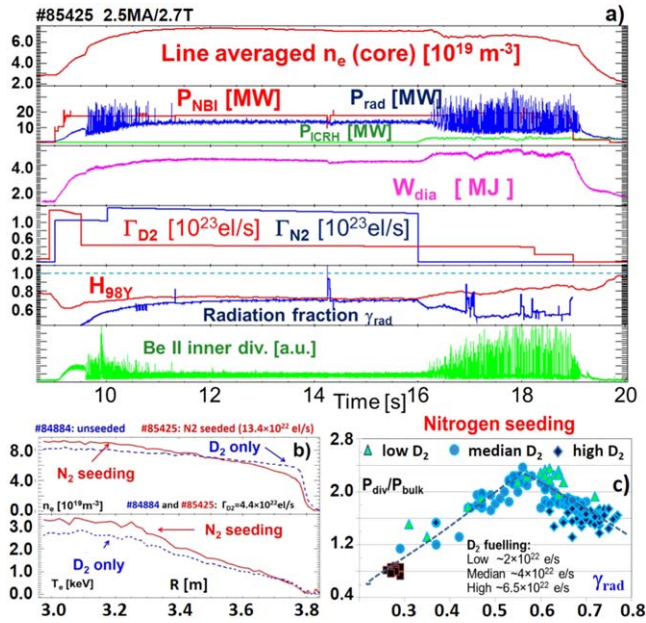


Figure 1 (a) Time traces of central line averaged n_e , NBI and ICRH heating power as well as total radiated power, plasma stored energy, D_2 -fuelling and N_2 -seeding waveforms, γ_{rad} and $H_{98(y,2)}$ -factor, Bell fast emission signal in the inner divertor of a N_2 -seeded high-density H -mode plasma on JET-ILW (b) comparison of n_e and T_e profiles for nitrogen (c) the ratio of the divertor radiation to the bulk radiation.

TGLF simulations by a stabilizing effect on the ITG modes through dilution of the main ion density [19]. On the other hand, T_e increases with N_2 seeding over the entire profile. Consequently, the impurity seeding strongly affects the particle transport and confinement, whereby possibly increasing the plasma stored energy. In contrast to these experiments, the N_2 seeding in JET-ILW in high triangularity geometry demonstrates an enhanced energy confinement due to an improved pedestal [9]. Also the plasma performance improvement with nitrogen is observed on ASDEX Upgrade where the improvement is clearly related to the improved pedestal performance [20].

Figure 1(c) shows the ratio of the divertor radiation to the bulk radiation in the plasmas with injected N_2 . In this contribution, we use the definition of the divertor radiation, $P_{\text{rad}}^{\text{div}}$, as the total radiation which is emitted below a height of $Z \leq -1.0 \text{ m}$ (for definition of the coordinate Z see figure 3), and $P_{\text{rad}}^{\text{bulk}} = P_{\text{rad}}^{\text{tot}} - P_{\text{rad}}^{\text{div}}$. This definition is commonly used on many existing machines [21, 22]. The reason for using this definition is as follows. The determination of the total power radiated below the X-point is not trivial, since the spatial resolution of the bolometer system on JET is not sufficient to determine whether radiation originates from inside or outside the separatrix. This is particularly problematic when emission radiation profiles have a peak in the vicinity of the X-point. For the characterisation of the radiation distribution, we are using here the ratio of radiation fractions in divertor and main chamber ($P_{\text{rad}}^{\text{div}}/P_{\text{rad}}^{\text{bulk}}$). This evaluated ratio, as well as $\gamma_{\text{rad}}^{\text{div}}$, does not demonstrate an obvious dependence on D_2 -fuelling in N_2 -seeded, type-I ELMy H -mode pulses. The fraction of the divertor radiation increases initially

with increase of the radiation fraction and reach the maximal value at $\gamma_{\text{rad}} \sim 55\% - 60\%$. Additional increase of γ_{rad} leads to a reduction of the $P_{\text{rad}}^{\text{div}}/P_{\text{rad}}^{\text{bulk}}$ indicating some level of saturation in the divertor radiation.

2.2. Ne and Ar seeding in high density H-mode plasmas

In addition to N_2 seeded scenarios, high radiation plasma scenarios with Ne and Ar seeding were investigated at JET. Neon is an auspicious candidate as a radiating impurity for plasma scenarios in the future reactors radiating effectively in the plasma edge at temperatures of $\approx 50 \text{ eV}$ [15].

As is discussed in [3], Ar and Ne seeding increased the total radiation fraction up to a level of $\gamma_{\text{rad}} \approx 63\%$ which is below the highest achieved radiated power fraction in N_2 seeded plasmas (75%). The radiation distribution inclined somewhat more biased towards the plasma core with radiation fraction of $\gamma_{\text{rad}}^{\text{div}} \approx 0.5$ in the divertor area, as one might expect from the electron temperature dependence of the radiative cooling efficiency function [15]. Contrary to N_2 seeding which leads to a significant improvement of the plasma energy confinement, the Ar injection causes only a moderate enhancement. Ne and Ar radiate as well in the pedestal region and main plasma (respectively) decreasing the power entering the scrape-off-layer (SOL) and consequently lowering the pedestal confinement [3, 5]. It was observed that Ar seeding prompts an $H-L$ transition at radiation fraction γ_{rad} of $\approx 60\%$ [3].

As demonstrated in detail in [3], the discharges with Ne injection showed beyond the radiation level of $\gamma_{\text{rad}} \approx 50\%$ an ELM-free phase (M -mode, as defined above) with a dithering between H - and L -mode (sequences of $H-L-H$ transitions). During the transient L -mode periods of these transitions, the γ_{rad} rises up to 95%, whereas the electron density is going down in the edge and in the core. The radiation profiles demonstrate divergent behaviours during the transition cycles as reported in [3]: during the L -mode period, the radiation pattern is located around the X-point with strong contributions in the inner and outer SOL; during the H -mode phase (or M -mode), the radiation profile is peaked in the zone above the X-point within the separatrix. During the ELM-free H -mode (or M -mode) phases with Ne seeding, an improvement of the confinement factor up to $H_{98(y,2)} \approx 0.75$ at $\gamma_{\text{rad}} \sim 50\%$ is observed. At the same time, the ion effective charge Z_{eff} is increasing by $\approx 80\%$ (increase of $\Delta Z_{\text{eff}} = 0.9$ to the value of $Z_{\text{eff}} = 2.0$ for the duration of the seeding) in Ne seeded plasmas in comparison with unseeded plasma ($Z_{\text{eff}} = 1.1$).

2.3. Combined N_2 and Ne seeding in H-mode plasmas

A detailed study of the synergistic effects of combined impurity injections is required to predict the practicality of such highly radiating scenarios to future fusion devices. Figure 2 shows the time traces of the plasma parameters in the plasma discharge with a combined gas seeding of N_2 and Ne. The discharge ($I_p/B_T = 2.5 \text{ MA}/2.7 \text{ T}$) is carried out in a vertical target divertor geometry at a low triangularity

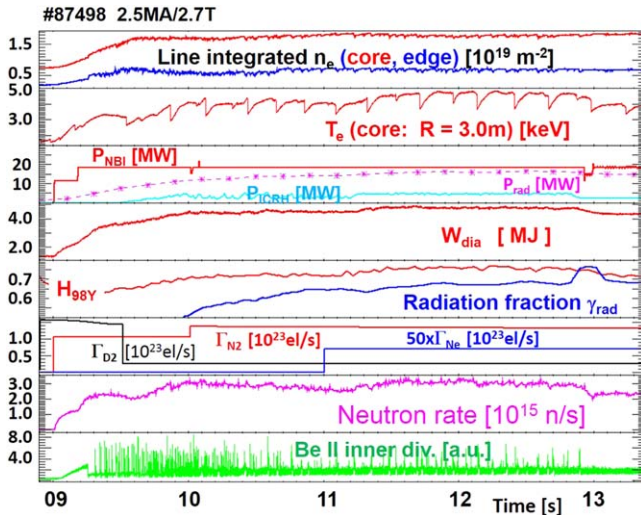


Figure 2. Time traces of combined $N_2 + Ne$ seeded ELMy H -mode discharge in JET-ILW (#87498). From top: line-integrated core and edge electron density measured by interferometer, T_e at $R = 3.0$ m measured by the ECE diagnostic, NBI and ICRH heating power as well as total radiated power, diamagnetic stored energy, $H_{98(y,2)}$ confinement factor and γ_{rad} , D_2 -fuelling and N_2 - and Ne -seeding waveforms, neutron rate, Be II fast emission signal in the outer divertor.

configuration ($\delta_{av} \approx 0.23$). NBI and ICRH heating powers were 18.5 MW and 4.5 MW respectively to maintain the plasma stored energy (W_{dia}) of 4.8 MJ. The nitrogen and neon are injected at the horizontal tiles into the PFR. The N_2 injection is started during the ramp-up phase in order to avoid the high heat loads on the divertor and to prevent W sputtering and its accumulation during this phase. The N_2 injection provokes the increase of the radiation fraction which reaches a quasi-stationary level of about 60% prior to the Ne injection phase ($Z_{eff} = 2.0$). Before the Ne seeding, the divertor is in a fully detached state and the normalized confinement following the ITER physics base scaling is around $H_{98(y,2)} = 0.71$ at about 80% of the Greenwald density. No significant heat flux is measured at the divertor targets. From $t = 11$ s, the small Ne gas puff is injected into the divertor (injection rate of $1.4 \times 10^{21} \text{ el s}^{-1}$). By adding a small amount of seeded Ne (seeded fraction of $\Gamma_{Ne}/\Gamma_{N_2} \approx 1\%$) to the N_2 puff, particle confinement and transport could be significantly improved. T_e rises in the plasma core without pedestal alteration. The electron temperature in the plasma core was measured by the electron cyclotron emission (ECE) diagnostic [23]. Z_{eff} increases during the combined seedings and reaches the value of 2.35 at $t = 13.0$ s. Additionally, figure 2 shows an improvement of the plasma stored energy during the combined seeding phase. As a result, applying a combination of nitrogen and neon gas seeding (11.4–13 s), good confinement ($H_{98(y,2)} = 0.78$) with high radiation fraction ($\gamma_{rad} = 0.7$) was reached in high density Type-I ELMy H -mode.

Also a slight increase of the neutron rate is observed during the phase with combined N_2 and Ne seeding. In the plasmas studied here, the neutrons are primarily created by the interaction of the NBI beams with the thermal deuterons.

This result is in agreement with the experimental observations reported in [19] where the neutron rate increases with increased neon puffing in the experiments under experimental conditions similar to those reported here.

Figure 3 shows the radiation distributions and the vertical Z -averaged radiation distributions for H -mode plasmas with N_2 seeding only as well as for combined N_2 and Ne seeding. The tomographically reconstructed radiation distribution shows intense radiation in the vicinity of the X-point for N_2 seeded plasmas as well as for plasmas with combined impurities injection. This observation is consistent with the statement given in [24] where it is reported that for conductive parallel heat flow, the plasma radiation in the scrape-off layer will peak in the region of the largest parallel temperature gradients. The largest parallel T_e -gradients are expected close to the divertor and around the X-point. It should be noted, however, that it is very likely that the radiation-associated heat sink leads to the formation of a steep parallel temperature gradient. The radiation distribution extends from the X-point peak its ‘wing-like’ pattern upwards along the separatrix towards the outside and inside mid-plane positions. As can be seen, it decreases strongly as one departs from the divertor. These findings are in agreement with the expected parallel T_e -gradient along the scrape-off layer. The electron temperature measured by Langmuir probes in the vicinity of the outer strike point during the combined impurity seeding reduces to 5 eV, which is the sensitivity level of the Langmuir probes. The inner target reaches these low temperatures earlier confirming the typical divertor asymmetry: a colder inner divertor region in comparison to the outer divertor leg. At the same time the total inner and outer saturation current exhibits a strong drop during the seeding, indicating that both targets are completely detached.

Adding a small amount of seeded Ne (seeded fraction of $\Gamma_{Ne}/\Gamma_{N_2} \approx 1\%$) increased strongly the radiation around X-point (figure 3) without altering the radiation in the main chamber as shown in the vertical Z -averaged radiation distribution (figure 3(a)). The increased seeded fraction to $\Gamma_{Ne}/\Gamma_{N_2} \approx 4\%$ at the middle seeding rate ($\Gamma_{N_2} \approx 7.6 \times 10^{22} \text{ el s}^{-1}$) increased significantly the X-point radiation and only moderately the core radiation (figure 3(b)) without visible impact on the energy confinement.

2.4. Combined N_2 and Ar seeding in H -mode plasmas

The radiation enhancement in the SOL region is more pronounced for the lower-Z atoms such as N_2 and Ne compared to Ar. The cooling efficiency of Ar reaches peak values at $T_e \sim 20$ eV and ~ 200 eV compared with that of N and Ne ions, which has a peak at 20–50 eV [15]. It is worth mentioning that the cooling efficiency of Ar is higher than that of Ne and N_2 . Correspondingly, argon reveals the highest radiative efficiency for the electron temperature range expected in the divertor region. Due to its high radiation losses in the core plasma, however, no high argon concentrations are permitted unless a very high compression in the divertor can be achieved [10]. Combined gas seeding of N_2 and Ar gas seeding was investigated in high density H -mode discharges. Figure 4 shows the

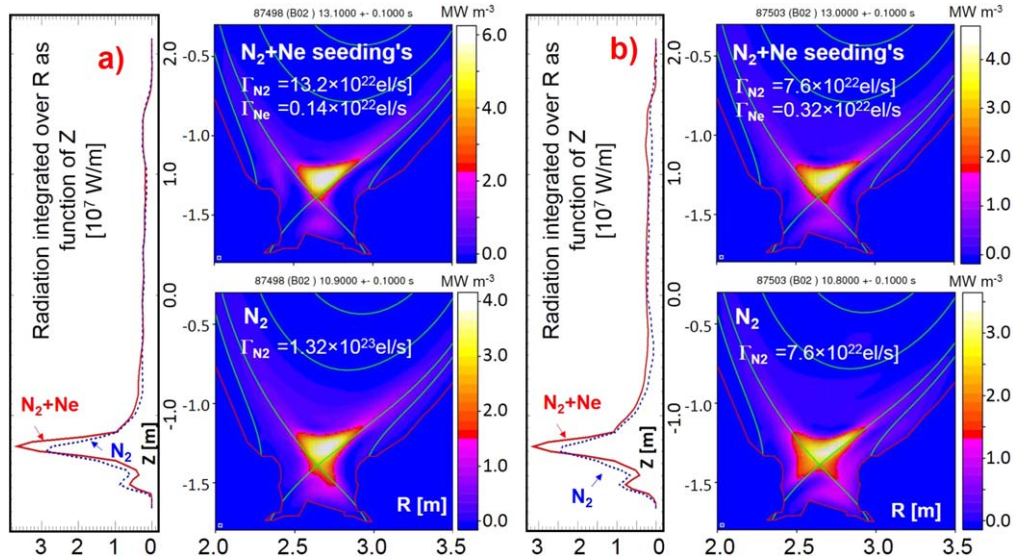


Figure 3. The vertical Z -averaged radiation distribution as well as tomographic reconstructions of the bolometric data for N_2 seeded as well as for the simultaneous N_2 and Ne injections. Figures (a) and (b) represent the cases with different impurity seeding rates as well as with different Γ_{Ne}/Γ_{N_2} ratios. During the combined impurity seeding, Z_{eff} reaches the values of 2.32 (figure 3(b)) and 2.35 (figure 3(a)) (figure 3(b)).

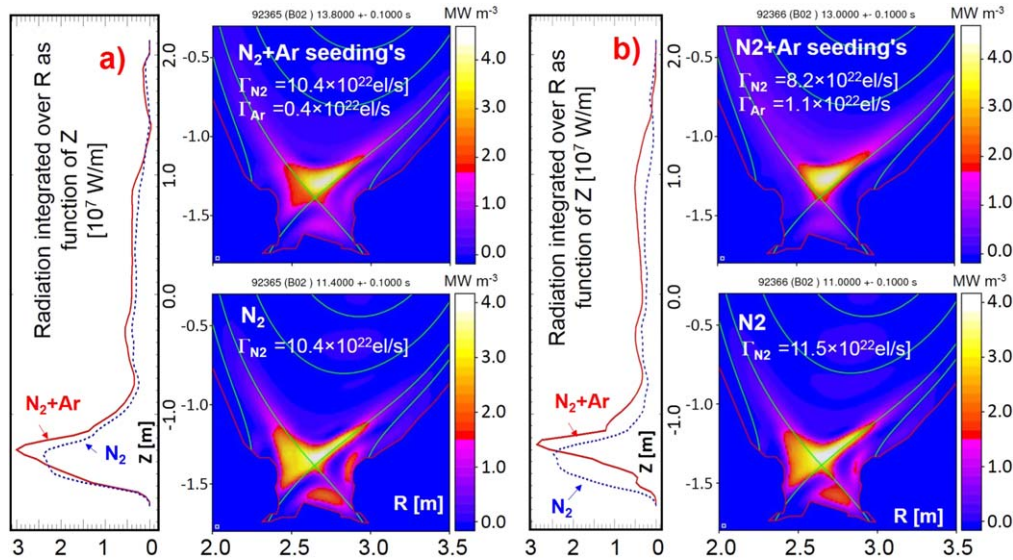


Figure 4. The vertical Z -averaged radiation distribution as well as tomographic reconstructions of the bolometric data for N_2 seeded and for the simultaneous N_2 and Ar injections. Figures (a) and (b) represent the examples with different impurity seeding rates as well as with different Γ_{Ar}/Γ_{N_2} ratios.

radiation distributions and the vertical Z -averaged radiation distributions for H -mode plasmas with N_2 seeding only as well as for combined N_2 and Ar injection. The nitrogen and Ar are injected (see figure 4(a)) at constant seeding rates of $\Gamma_{N_2} \approx 1.04 \times 10^{23} \text{ el s}^{-1}$ ($8.2 \times 10^{22} \text{ el s}^{-1}$ in figure 4(b)) and $\Gamma_{Ar} \approx 0.41 \times 10^{22} \text{ el s}^{-1}$ ($1.1 \times 10^{22} \text{ el s}^{-1}$ in figure 4(b)) which corresponds to the impurity seeded mixed fraction of $\Gamma_{Ar}/\Gamma_{N_2} \approx 4\%$ (13% in figure 4(b)). For both cases, with N_2 only seeding ($Z_{eff} \approx 1.85$) as well as with combined N_2 and Ar injections ($Z_{eff} \approx 2.15$ (figure 4(a)) and $Z_{eff} \approx 2.3$ (figure 4(b))), the predominant radiation comes from the confined area and is located in a region near the X -point. Nevertheless, in contrast to

combined impurity puffing, the radiation in the inner divertor is clearly visible for the plasma with N_2 cooling alone. From the X -point peak, the radiation distribution with combined impurity injections extends much strongly the ‘wings-like’ pattern upwards along the separatrix towards the inside and outside mid-plane positions. These radiation patterns reveal a clear in-out asymmetry. It could be explained by the strong poloidal asymmetry of the distribution of injected impurity ions. The impurity poloidal distribution in the plasma edge was intensively studied in [25] where the simulation with B2SOLPS5.2 transport code predicts a strong poloidal asymmetry. The asymmetry is explained by neoclassical effects in a plasma with strong

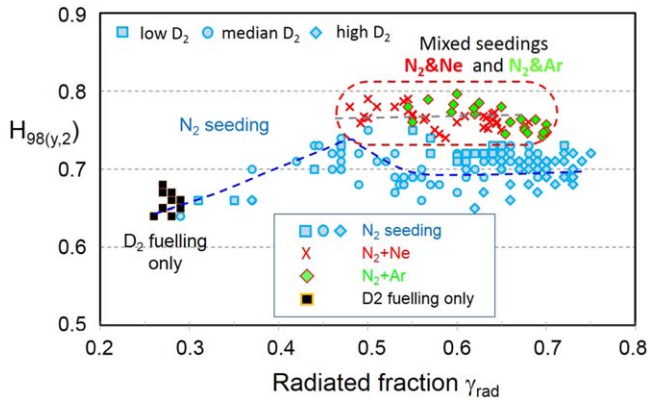


Figure 5. $H_{98(y,2)}$ as a function of radiated power fraction. Improved confinement for combined $N_2 + Ne$ as well as $N_2 + Ar$ radiators is approached in high density, highly radiative H -mode plasma scenarios.

gradients [25]. A significant increase of the radiation in the main plasma (P_{rad}^{bulk}) can be clearly seen in the vertical Z -averaged radiation distributions (figures 4(a), (b)): the increase of about 50% from 7.2 to 10.9 MW for the case shown in figure 4(a) and the rise of $\approx 75\%$ from 6.2 to 10.8 MW in the case of figure 4(b). These vertical distributions (figures 4(a), (b)) do not show any significant improvement in the peak divertor radiation. It should be noted here that the radiation pattern in the PFR in figure 4 is an artifact, which are arising from the problem of non-perfect covering of the JET bolometry system of the corner region in the outer divertor leg.

On the other hand, the location of maximum radiation moves to the direction of the main chamber. These results are consistent with tomographic reconstructions of the radiation distributions: in the combined seeding scenario ($N_2 + Ar$) radiation ‘spills over’ into the area above the X -point inside of the separatrix.

3. Confinement in high-density highly radiative H -mode plasma scenarios

With regard to future fusion devices, the effect of various seed impurities on the plasma confinement needs to be investigated. Figure 5 shows the confinement factor $H_{98(y,2)}$, measured during the experiments with three seeded impurity species N_2 , Ne and Ar , as a function of radiated power fraction. The plasma performance in the N_2 seeded plasmas was analysed over a deuterium fuelling range of $2 \times 10^{22} \text{ el s}^{-1} \div 6.5 \times 10^{22} \text{ el s}^{-1}$ and an impurity seeding range of $2 \times 10^{22} \text{ el s}^{-1} \div 1.3 \times 10^{23} \text{ el s}^{-1}$. The confinement increases from $H_{98(y,2)} = 0.65$ in unseeded pulses with $\gamma_{rad} \sim 30\%$ to a value of $H_{98(y,2)} = 0.75$ at $\gamma_{rad} \sim 50\%$ with N_2 injection.

As it is discussed in section 2.1, the N_2 seeding significantly affects the particle confinement and transport increasing the energy stored in the plasma: the degraded electron density pedestal is accompanied by an n_e increase in the plasma core as well as an increase of the electron temperature T_e in the core. Further increase of γ_{rad} with increase of the N_2 seeding rate leads to a moderate confinement

degradation. Beyond $\gamma_{rad} \sim 55\%$, the energy confinement scaling factor remains almost constant at ≈ 0.7 .

The confinement improvement during the N_2 seeding in JET-ILW is in contrast to findings seen in JET-C with a carbon divertor, where a reduction of $H_{98(y,2)}$ was always observed during impurity seeding [26, 27]. Comparison of the thermal energy confinement for the unseeded discharges as well as for three seeding scenario cases is shown in figure 5. This figure demonstrates the further enhancement of the plasma performance for the radiation fractions beyond 55%. The maximum value of $H_{98(y,2)} = 0.78$, reached at combined $N_2 + Ne$ and $N_2 + Ar$ impurity injections, is lower than required for ITER. It should be noted, however, that the unseeded discharges have already a low confinement factor $H_{98(y,2)}$ of about 0.65. Therefore, the impurity seeded ELMy H -mode discharges allow operation at higher densities compared to unseeded reference discharges, with good confinement or at least without a strong degradation of the confinement, as illustrated in figure 5.

4. Conclusion

To find the optimum proportion of multiple seeded impurity species (Ne , Ar , N_2) compatible with a high confinement, dedicated H -mode impurity seeding experiments with different mixtures of seeded impurities have been performed in JET-ILW. We investigated how different mixtures influence the radiation patterns, radiation distributions as well as the confinement in the divertor and in the plasma core. The nitrogen causes a considerable energy confinement recovery from a confinement factor of $H_{98(y,2)} \approx 0.65$ in the discharge with D_2 fuelling only to a factor of $H_{98(y,2)} \approx 0.75$ at $\gamma_{rad} \sim 50\%$. Further increase of γ_{rad} with increase of the N_2 seeding rate leads, however, to a moderate confinement degradation. These losses of the plasma performance for the radiation fractions beyond 55% can be recovered by applying of combined $N_2 + Ne$ and $N_2 + Ar$ impurity injections. The confinement factor increased from 0.7 with N_2 seeding to the value of $H_{98(y,2)} = 0.78$ ($N_2 + Ne$ or $N_2 + Ar$ seeding). By adding a small amount of seeded Ne (seeded fraction of $\Gamma_{Ne}/\Gamma_{N_2} \approx 1\%$) to the N_2 puff, particle confinement and transport is significantly affected. T_e rises in the plasma core without pedestal alteration. As a result, the energy stored in the plasma and the confinement factor are increased to $H_{98(y,2)} \approx 0.78$. Also a good confinement of $H_{98(y,2)} \approx 0.77$ at a seeded fraction of $\Gamma_{Ar}/\Gamma_{N_2} \approx 4\%$ has been demonstrated regardless of significant radiation from inside the separatrix.

There is an intense radiation in the vicinity of the X -point for N_2 seeded plasmas as well as for plasmas with injection of combined impurities. The small seeded fraction of $\Gamma_{Ne}/\Gamma_{N_2} \approx 1\%$ increased strongly the radiation around X -point without altering the radiation in the main chamber. On the other hand, the increased seeded fraction to $\Gamma_{Ne}/\Gamma_{N_2} \approx 4\%$ improved notably the X -point radiation and only moderately the radiation in the plasma core. The radiation distribution with combined $N_2 + Ar$ impurity injections extends much strongly the ‘wings-like’ pattern upwards along

the separatrix towards the inside and outside mid-plane positions. At this impurity mix, a pronounced increase of the radiation in the main plasma has been observed. These experiments with combined impurity seeding show that an increase of the radiation inside the separatrix has no impact on the energy confinement. Additionally, it is demonstrated that the X-point radiation in the JET-ILW is stable, reproducible and reversible.

Based on the result of this contribution, a mix of impurities could be considered for ITER and DEMO, a low-Z impurities for divertor radiation and a medium-Z impurities for radiation in the confined region to optimize the heat flux removal to the first wall by radiation in the divertor region and in the main plasma chamber. However, it should be noted that in contrary to JET, ITER will operate very close to the L - H power threshold. Therefore, an increase of the pedestal radiation seems to bear higher risks for triggering in ITER the back transition from H to L mode. This might hinder the mid-Z radiator applicability. In ITER the ‘natural’ radiation from intrinsic impurities, He and Bremsstrahlung is expected to be around 30% of the total loss power from the plasma, $P_{\text{loss}} = P_{\text{heat}} - dW/dt$, and thus no further reduction of the power flux across the separatrix is required in the standard ITER scenarios. But if ITER scenarios would require lower target heat loads for risk mitigation, then the mid-Z may be needed. On the other hand, the DEMO fusion reactor has to dissipate $\approx 70\%$ of the total heating power (of around 450 MW [28]), to be radiated inside the separatrix and, therefore, a mid-Z impurity is required [5].

Acknowledgments

This work has been carried out within the framework of the EUROfusion Consortium and has received funding from the Euratom research and training programme 2014–2018 and 2019–2020 under grant agreement No 633053. The views and opinions expressed herein do not necessarily reflect those of the European Commission.

ORCID iDs

A Huber  <https://orcid.org/0000-0002-3558-8129>
 S Wiesen  <https://orcid.org/0000-0002-3696-5475>
 S Brezinsek  <https://orcid.org/0000-0002-7213-3326>
 V Huber  <https://orcid.org/0000-0002-5213-1841>
 Ch Linsmeier  <https://orcid.org/0000-0003-0404-7191>
 Ph Mertens  <https://orcid.org/0000-0002-5010-5316>

References

- [1] Loarte A et al 2007 *Nucl. Fusion* **47** S203–63
- [2] Raffray A R et al 2010 *Fusion Eng. Des.* **85** 93–108
- [3] Huber A et al 2014 Impact of strong impurity seeding on the radiation losses in JET with ITER-like Wall *Proc. 41th EPS Conf. on Controlled Fusion and Plasma Physics (Berlin, Germany, 23–27 June)*
- [4] Bernert M et al 2017 *Nucl. Mater. Energy* **12** 111–8
- [5] Wischmeier M et al 2015 *J. Nucl. Mater.* **463** 22–9
- [6] Oberkofler M et al 2013 *J. Nucl. Mater.* **438** S258–61
- [7] Kukushkin A S et al 2011 *Fusion Eng. Des.* **86** 2865
- [8] Reinke M L et al 2011 *J. Nucl. Mater.* **415** S340–4
- [9] Giroud C et al 2013 *Nucl. Fusion* **53** 113025
- [10] Kallenbach A et al 2013 *Plasma Phys. Control. Fusion* **55** 124041
- [11] Asakura N et al 2009 *Nucl. Fusion* **49** 115010
- [12] Kallenbach A et al 2012 *Nucl. Fusion* **52** 122003
- [13] Matthews G F et al 2011 *Phys. Scr.* **T145** 014001
- [14] Brezinsek S et al 2013 *J. Nucl. Mater.* **438** S303–8
- [15] Post D et al 1995 *Phys. Plasmas* **2** 2328
- [16] Greenwald M 2002 *Plasma Phys. Control. Fusion* **44** R27
- [17] Solano E R et al 2017 *Nucl. Fusion* **57** 022021
- [18] Pasqualotto R et al 2004 *Rev. Sci. Instrum.* **75** 3891
- [19] Gloeggler S et al 2019 *Nucl. Fusion* **59** 126031
- [20] Schweinzer J et al 2011 *Nucl. Fusion* **51** 113003
- [21] Fuchs J C et al 2001 *J. Nucl. Mat.* **290–293** 525
- [22] Ingesson L C et al 2002 Radiation in impurity-seeded discharges in the JET MkI, MkIIA & MkII GB divertors *EFDA-JET-CP (02)01/11 PSI Conference (Japan, 22–31 May)*
- [23] de la Luna E et al 2004 *Rev. Sci. Instrum.* **75** 3831
- [24] Pitcher C S and Stangeby P C 1997 *Plasma Phys. Control. Fusion* **39** 779
- [25] Rozhansky V et al 2015 *Nucl. Fusion* **55** 073017
- [26] Maddison G et al 2011 *Nucl. Fusion* **51** 042001
- [27] Giroud C et al 2012 *Nucl. Fusion* **52** 063022
- [28] Zohm H et al 2013 *Nucl. Fusion* **53** 073019